$\delta^{13}C$ values of bacterial hopanoids and leaf waxes as tracers for methanotrophy in peatlands

Gordon N. Inglis[a], B. David A. Naafs[a], Yanhong Zheng[b], Judith Schellekens[c], Richard D. Pancost[a] and the 'T-GRES Peat Database collaborators'

[a] Organic Geochemistry Unit, School of Chemistry, School of Earth Sciences, and Cabot Institute, University of Bristol, Bristol, UK

[b] State Key Laboratory of Continental Dynamics, Department of Geology, Northwest University, Xi'an, PR China

[c] Department of Soil Science, University of São Paulo, Piracicaba, Brazil

Corresponding author: Gordon N. Inglis

Email: gordon.inglis@bristol.ac.uk. Telephone: +44 (0)117 954 6395

Abstract

Methane emissions from peatlands contribute significantly to atmospheric CH_4 levels and play an essential role in the global carbon cycle. The stable carbon isotopic composition ($\delta^{13}C$) of bacterial and plant lipids has been used to study modern and past peatland biogeochemistry, especially methane cycling. However, the small number of recent peatlands that have been characterised and the lack of consistency between target compounds means that this approach lacks a rigorous framework. Here, we undertake a survey of bacterial and plant lipid $\delta^{13}C$ values in peatlands from different geographic regions, spanning a wide range of temperature (-8 to 27°C) and pH (~3 to 8), to generate a reference dataset and probe drivers of isotopic variability. Within our dataset, the carbon fixation pathway predominantly determines leaf wax (*n*-alkane) $\delta^{13}C$ values. Bacterial-derived C_{31} hopane $\delta^{13}C$ values track those of leaf waxes but are relatively enriched (0 to 10‰), indicating a heterotrophic ecology and preferential consumption of ^{13}C-enriched substrates (e.g. carbohydrates). In contrast, ≤ C_{30} hopanoids can be strongly ^{13}C-depleted and indicate the incorporation of isotopically light methane into the bacterial community, especially at near neutral pH (~5-6 pH). Previous analysis of Eocene sediments has suggested isotopic decoupling between C_{31} and ≤ C_{30} hopanoid $\delta^{13}C$ values. Our work suggests a globally widespread decoupling in recent peatlands; this persists despite the profound diversity of hopanoid producing bacteria and associated controls on their $\delta^{13}C$ values and it has significant implications for future work. Re-analysis of published data from: 1) the (mid-to-early) Holocene and late Glacial, and 2) latest Paleocene and earliest Eocene in this revised context highlights that perturbations to the peatland methane cycle occurred during the past, and we envisage that this approach could provide unique (qualitative) insights into methane cycling dynamics throughout the geological record.

1. Introduction

Wetlands play an essential role in the global carbon cycle and are one of the largest carbon stores on land (> 600 PgC) (Yu et al., 2010). They are also the largest natural source of atmospheric methane (CH_4) (Dean et al., 2018), with current emissions ranging between 55 and 230 Tg CH_4 yr^{-1} (Turetsky et al., 2014). Increasing (tropical) wetland CH_4 emissions could also be responsible for the unexpected increase in atmospheric CH_4 concentrations since 2007 (Nisbet et al., 2016). This could have implications for tackling future global warming and highlights the importance of understanding wetland methane cycling during past warm climates.

Temperature, hydrology, pH and vegetation primarily govern wetland CH_4 emissions (Bridgham et al., 2013; Turetsky et al., 2014). CH_4 emissions are further regulated by the interplay between methanogenesis and methanotrophy, all of which are controlled by a range of physical, biological and chemical processes (Segers, 1998). These disparate processes will exert complex controls on the stable carbon isotopic composition ($\delta^{13}C$) of wetland organic matter, which when untangled could serve as powerful tools for reconstructing the carbon cycle and microbial ecology in modern and ancient wetlands.

Plant (e.g. leaf wax) $\delta^{13}C$ values are governed by the concentration and carbon isotopic composition of ambient CO_2 (which can deviate from atmospheric values), relative humidity and vegetation type (Collister et al., 1994; Diefendorf et al., 2011; Farquhar et al., 1989). However, plant $\delta^{13}C$ values can also be influenced by aerobic methanotrophy. Previous studies indicate that ^{13}C-depleted CH_4 can be converted to carbon dioxide (CO_2) within the water-filled hyaline cells of *Sphagnum* moss and subsequently incorporated into biomass (Kip et al., 2010; Raghoebarsing et al., 2005) and plant lipids such as phytosterols (up to -32‰; Elvert et al., 2016; Liebner et al.,

2011) and mid-chain C_{21}-C_{25} *n*-alkanes (e.g. C_{23} *n*-alkane: up to -43‰; Elvert et al., 2016; van Winden et al., 2010). As such, the occurrence of ^{13}C-depleted plant lipids in wetland environments could be a useful tool to reconstruct *Sphagnum*-associated methanotrophy. However, more ground truthing is needed to upscale this approach globally.

The interplay of plant biomass $\delta^{13}C$ values, heterotrophy and methanotrophy will also govern the $\delta^{13}C$ values of bacterial-derived hopanoid biomarkers. Hopanoids are produced by a wide range of bacteria (Talbot and Farrimond, 2007; Talbot et al., 2016b) and $\delta^{13}C$ values of the C_{31} hopane range from -22 to -26‰ in recent wetlands (Pancost et al., 2003; Xie et al., 2004). This indicates a predominantly heterotrophic source (Pancost and Sinninghe Damsté, 2003; Pancost et al., 2000) and supports previous studies that have shown that the majority of precursor organisms biosynthesising hopanoids in peat-forming environments are heterotrophs (see Talbot et al., 2016a and ref. therein). Methanotrophy appears (perhaps unexpectedly) to be a minor control on hopanoid $\delta^{13}C$ values. However, recent work on a limited set of recent wetland samples has shown that C_{30} hopenes can yield lower values (e.g. -up to -38‰; van Winden et al., 2010; Zheng et al., 2014). Low C_{30} hopene $\delta^{13}C$ values (up to -60‰) have also been identified in lacustrine settings (Davies et al., 2015; Naeher et al., 2014), indicating incorporation of isotopically light CH_4 into the bacterial community. As C_{30} hopenes are produced by a variety of organisms (including methanotrophs; e.g. Rohmer et al., 1984), these compounds may be suitable candidates for tracking changes in wetland CH_4 cycling. However, due to the small number of recent wetlands that have been studied, as well as a lack of consistency between target compounds and the narrow range of wetland diversity sampled, our

understanding of the impact of methanotrophy upon hopanoid $\delta^{13}C$ values in wetland - and hence the CH_4 cycle - remains limited.

Here we undertake a survey of *n*-alkane and hopanoid $\delta^{13}C$ values from the upper meter of sediment in a range of peatlands (n = 199 samples from 37 peatlands in boreal, temperate and tropical regions), spanning a wide range of temperature (-8 to 27°C), pH (~3 to 8) and vegetation. We focus on peatlands as these contribute significantly to atmospheric CH_4 levels. We use this to generate a reference dataset and assess the controls on *n*-alkane (C_{21} to C_{33}) and hopane/hopene (C_{27} to C_{32}) $\delta^{13}C$ values, including heterotrophy, methanotrophy, temperature, pH and vegetation. Guided by these results, we use our dataset to re-interpret previously published hopanoid and *n*-alkane $\delta^{13}C$ values from the mid-to-early Holocene and late Glacial (4 to 18 thousand years ago) and early Eocene and latest Paleocene (48 to 56 million years ago) and use these new interpretations to constrain the operation of the CH_4 cycling during the past.

2. Methods

2.1. Peat material

To expand the existing data and build a significantly larger database of hopanoid and *n*-alkane $\delta^{13}C$ values, we analysed samples from a subset of the peatland database we developed previously (Naafs et al., 2017). This includes samples (n = 157) from 34 peatlands from boreal (Iceland, Finland, Norway, Sweden, Russia), temperate (Argentina, Canada, USA, Germany, Iceland, Iran, Spain) and tropical (Brazil, Peru, Indonesia, Kenya)-geographic locations (Fig. 1; SI Appendix). Samples (n = 42 from 3 sites) were also compiled from published studies (van Winden et al., 2012b; Xie et al., 2004; Zheng et al., 2014).

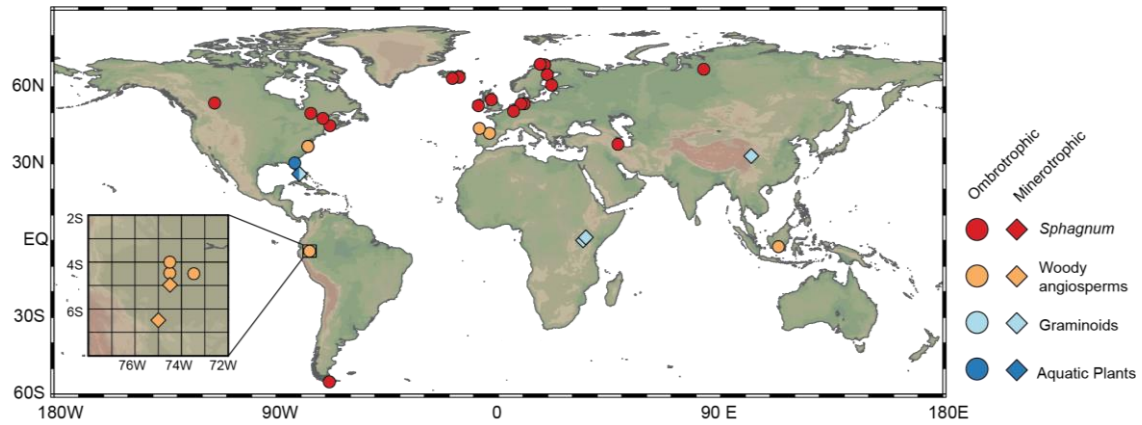

Figure 1. Map with the location of all recent peatlands used in this study.

124

125 2.1.1. Sampling approach

126 Samples for the reference dataset (n = 199; section 2.1) were collected from different
127 horizons within the top 50 to 100cm of peat. Our dataset includes: 1) surface samples,
128 2) samples above and below the acrotelm/catotelm boundary and 3) samples
129 distributed throughout the peat. This approach allows us to assess both spatial and
130 downcore variability. Our dataset also spans important biogeochemical gradients (e.g.
131 acrotelm/catotelm boundary).

132 Variations in peat accumulation rates differ between sites, implying that the age
133 of lipid biomarkers (and their $\delta^{13}C$ values) might differ. However, the available age
134 models indicate that the top 100cm of peat in our reference dataset range between
135 800 to 2000 years in age (Chambers et al., 2014; De Vleeschouwer et al., 2012;
136 Lähteenoja et al., 2009; Page et al., 2004; Rydberg et al., 2010; Väliranta et al., 2007;
137 Xie et al., 2004; Zheng et al., 2014). For sites without an age model, we use published
138 accumulation rates (Aaby and Tauber, 1975; Gorham, 1991; Page et al., 2004;
139 Sorensen, 1993) to estimate the approximate time interval captured by 100 cm of peat
140 deposition. These estimates strongly suggest that the majority of our sites (all of which
141 are < 100cm, and typically < 60cm) span the last 2000 years. Crucially, this means

that our compilation reflects recent rather than modern processes. Hereafter, the data obtained from these upper 100 cm will be referred to as our “recent” reference dataset.

2.2. Environmental parameters

Environmental parameters (e.g. latitude, longitude, altitude, mean annual air temperature, pH and vegetation) were obtained for each site. This data is included within the supplementary information. Mean annual air temperature (MAAT) and altitude were calculated using the simple bioclimatic model PeatStash, which computes MAAT and altitude globally with a 0.5-degree spatial resolution (see Naafs et al., 2017). Directly measured pH data was used as reported (Naafs et al., 2017; Huang et al., 2018). Vegetation information was obtained from published studies (Broder and Biester, 2015; De Vleeschouwer et al., 2012; Huang et al., 2018; Jauhiainen et al., 2005; Lähteenoja and Page, 2011; Mauquoy et al., 2004; Pancost et al., 2011; Pancost et al., 2000; Souto et al., 2016; Souto et al., 2017; Zheng et al., 2014) or via personal communication (L. Rochefort, F. De Vleeschouwer, A. Rizzuti, A. Gallego-Sala, A. Sharifi, R. Bindler, L. Gandois). Each peatland is characterised by a wide variety of plants, including mosses, woody angiosperms, woody gymnosperms, graminoids and aquatic plants; as such, we have classified sites based upon the dominant plant type in each setting (see Fig. 1; SI Appendix). However, we note that other types of plants can be present and can be dominant in some depth intervals. There are also other parameters that may be important but are not considered here due to the methodological design (e.g. hydrology, substrate availability and microbial ecology).

166 *2.3. Organic Geochemistry*

167 2.3.1. Extraction and separation

168 New peat material (see section 2.1) was extracted using an Ethos Ex microwave
169 extraction system using 15 ml of dichloromethane (DCM) and methanol (MeOH) (9:1,
170 *v/v*, respectively) at the Organic Geochemistry Unit in Bristol. These were all
171 previously extracted by Naafs et al. (2017). The microwave program consisted of a 10
172 min ramp to 70 °C (1000 W), 10 min hold at 70 °C (1000 W), and 20 min cool down.
173 Samples were centrifuged at 1700 rounds per minute for 3-5 min, and the supernatant
174 was removed and collected. A further 10 ml of DCM:MeOH (9:1, *v/v*) was added to the
175 remaining sample and centrifuged again, after which the supernatant was removed
176 and combined with the previously obtained supernatant. This process was repeated
177 3-6 times, depending on the volume of sample, to ensure that all extractable lipids
178 were retrieved. The total lipid extract (TLE) was initially separated over silica into
179 apolar and polar fractions using hexane:dichloromethane (9:1, *v/v*) and
180 dichloromethane:methanol (1:2, *v/v*), respectively. In some tropical peatlands (e.g.
181 Peru), an unknown pentacyclic triterpene methyl ether (Jacob et al., 2005) co-eluted
182 with the C_{31} ββ hopane. To enable subsequent $\delta^{13}C$ analysis of the C_{31} ββ hopane,
183 we therefore separated the apolar fraction over silica into a hydrocarbon and
184 aromatic/ether fraction using hexane (100%) and hexane:dichloromethane (3:1, *v/v*)
185 respectively.

186 Urea adduction was used to separate cyclic (i.e. non-adduct) and aliphatic (i.e.
187 adduct) hydrocarbons. This was performed on a subset of samples which contained a
188 wide range of hopanoid lipids. To achieve this, 200 µl of hexane, 200 µl of acetone
189 and 200 µl of urea (10% in MeOH) were successively added to the saturated
190 hydrocarbon fraction. The sample was frozen for ca. 60 minutes until urea crystals

formed. Solvent was then removed under a gentle stream of N_2 and the urea extracted (×5) with ca. 1 ml of *n*-hexane (cyclic fraction). The urea crystals were then dissolved in 500 µl of MeOH and 500 µl of water and the aliphatic fraction was extracted (×5) with ca. 1 ml of *n*-hexane. The adduction procedure was repeated on the adduct fraction once more to ensure all non-adduct material was removed (Pancost et al., 2008).

2.3.2 GC-MS analysis

Gas chromatography-mass spectrometry (GC-MS) was performed using a Thermo Scientific ISQ Single Quadrupole gas chromatography-mass spectrometer. Using helium as the carrier gas, 1 µl of sample (dissolved in hexane) was injected at 70 °C using an on-column injector. The temperature program included four stages: 70 °C hold for 1 min, 70–130 °C at 20 °C/min rate; 130–300 °C at 4 °C/min; and temperature hold for 20 min at 300 °C. The electron ionisation source was set at 70 eV. Scanning occurred between *m/z* ranges of 50–650 Daltons. The GC was fitted with a fused silica capillary column (50 m × 0.32 mm i.d.) coated with a ZB1 stationary phase (dimethylpolysiloxane equivalent, 0.12 µm film thickness). Hopanoids and *n*-alkanes were identified based upon published spectra, characteristic mass fragments and retention times (e.g. Van Dorsselaer et al., 1974, Rohmer et al., 1984, Uemura and Ishiwatari, 1995, Sessions et al., 2013).

2.3.3. GC-C-IRMS analysis

Gas chromatography-combustion-isotope ratio mass spectrometry (GC-C-IRMS) was performed using an Isoprime 100 GC-combustion-isotope ratio mass spectrometer system. Samples were measured in duplicate with a reproducibility of <0.5‰ and $\delta^{13}C$ values were converted to VPDB by bracketing with an in-house gas (CO_2) of known $\delta^{13}C$ value. The Instrument stability was monitored by regular analysis of an in-house standard; long-term precision is ± 0.3‰. Injection volume was 1 µl onto to a Zebron-I nonpolar column (50 m × 0.32 mm i.d., 0.10 µm film thickness). GC conditions were the same as described above for GC-MS analysis (see 2.3.2).

2.4. Statistical analysis

To assess the correlation between different lipid biomarker $\delta^{13}C$ values (e.g. C_{23} vs C_{25} *n*-alkanes) we calculated Pearson product correlation coefficients (r), residuals and probability plots. To determine whether two means are significantly different ($p < 0.05$), we used independent sample t-tests. To estimate the relationship between $\delta^{13}C$ lipid values and environmental parameters we calculated Deming regressions and calibration coefficients of determination (R^2) using the R software package (http://www.R-project.org/; see Inglis et al., 2018 for full code). Deming regressions differ from simple linear regressions as they consider the error on both the *x*- and *y*-axis (Adcock, 1878). Here, we assume that the error associated with proxy measurements and environmental parameters is independent and normally distributed. To calculate a Deming regression, we must define the standard deviation (σ) for both the *x*- and *y*-axis. For MAAT, the standard deviation is defined as 1.5 °C (see Naafs et al., 2017). For pH, the standard deviation is defined as 0.5 pH units (see Naafs et al., 2017). For the $\delta^{13}C$ lipid values, the standard deviation and ratio of

variance must also be defined. Residuals are used to evaluate the performance of the linear model and were calculated for the full dataset using the following equation:

$$Residual_y = y_{observed} - y_{predicted}$$

3. Results

3.1. n-alkane $\delta^{13}C$ values

Saturated hydrocarbon fractions (n = 199) contained the range of *n*-alkanes (C_{19}-C_{33}) typically found in such settings (Pancost et al., 2003; Quirk et al., 1984; Xie et al., 2004) and were dominated by mid-chain (C_{21} to C_{25}) and long-chain *n*-alkanes (C_{27} to C_{33}). Mid-chain *n*-alkane (C_{21}-C_{25}) $\delta^{13}C$ values average -33 ‰ and range from -27 to -39‰ (n = 286, σ = 2.0, skewness = - 0.4; Fig. 3). Long-chain *n*-alkane (C_{27}-C_{33}) $\delta^{13}C$ values average -32 ‰ and range from -28 to -38‰ (n = 621; σ = 1.8, skewness = -0.7; Fig. 2). Although the two *n*-alkane groups have similar carbon isotopic averages and ranges, the skewness and hence distribution profiles slightly differ. The $\delta^{13}C$ values of compounds derived from similar sources are expected to be linearly correlated and with slopes of 1. Significant linear correlations do exist between mid-chain (C_{21}-C_{25}) *n*-alkane $\delta^{13}C$ values (r = 0.73 to 0.90; p < 0.001; Supplementary Information) and between long-chain (C_{29}-C_{33}) *n*-alkane $\delta^{13}C$ values (r = 0.76 to 0.91; p < 0.001; Supplementary Information). However, the correlation between mid-chain (C_{21}-C_{25}) and long-chain (C_{29}-C_{33}) *n*-alkane $\delta^{13}C$ values is low (r = 0.07 to 0.29).

Within a single peatland, mid-chain *n*-alkanes exhibit minor variations in $\delta^{13}C$ values (σ = 0.6 to 1.6‰; Fig. S1-S2) and the average downcore variability (σ = 1.1‰) is significantly lower than the global range (σ = 3.0‰). Long-chain *n*-alkanes also exhibit minor variations in $\delta^{13}C$ values (σ = 0.7 to 2.0‰; Fig. S1-S2) and the average

downcore variability (σ = 1.0‰) is lower than the global range (average σ = 1.8‰). Consistent with previous studies (e.g. Xie et al., 2004), there is also no significant variation in long-chain and mid-chain *n*-alkanes $\delta^{13}C$ values between deep (>15 cm) and shallow (<15 cm) sections of the peat (Fig. S1-S2).

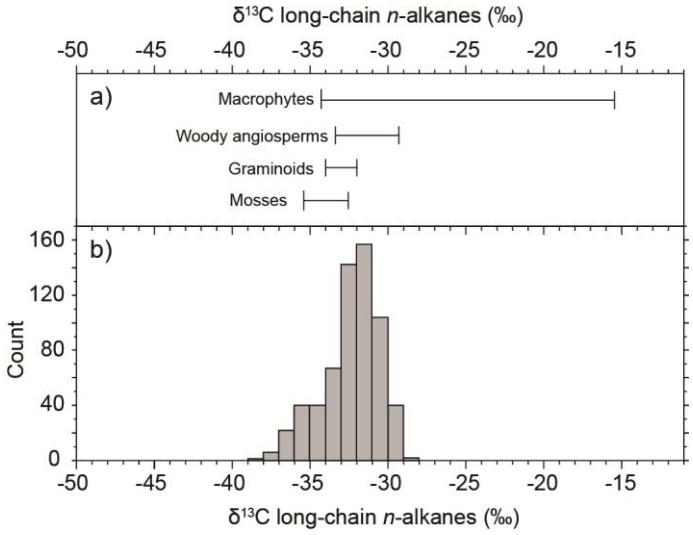

Figure 2. Compilation of long-chain (C_{27}-C_{33}) *n*-alkane $\delta^{13}C$ values in (a) modern peatland plants (Aichner et al., 2010, Brader et al., 2010, Ficken et al., 1998, Huang et al., 2010, Huang et al., 2012, Mead et al., 2005, van Winden et al., 2010, Xie et al., 2004) and (b) recent peatlands (*this study*). Peatland *n*-alkane $\delta^{13}C$ values reported from the upper 100 cm only.

3.2. Hopanoid $\delta^{13}C$ values

Saturated hydrocarbon fractions (n = 199) contained the range of hopanes and hopenes typically found in such settings (Pancost et al., 2003; Quirk et al., 1984; Xie et al., 2004) and are described in detail in Inglis et al. (2018). The C_{31} αβ hopane - one of the most abundant hopanoids in peat (Inglis et al., 2018) - yields an average $\delta^{13}C$ value of -26‰ with a range from -17 to -32‰ (n = 102, σ = 2.8, skewness = -0.49; Fig. 4). The average $\delta^{13}C$ value of the C_{31} ββ hopane is similar with a value of -26‰ (n =

61; σ = 3.8, skewness = -1.1; Fig. 4). $\delta^{13}C$ values of the C_{31} ββ and C_{31} αβ hopanes are positively correlated ($r = 0.87$; $p < 0.001$). There is also a linear correlation between $\delta^{13}C$ values of the C_{31} hopane (both αβ and ββ) and long-chain *n*-alkanes (Fig. S3).

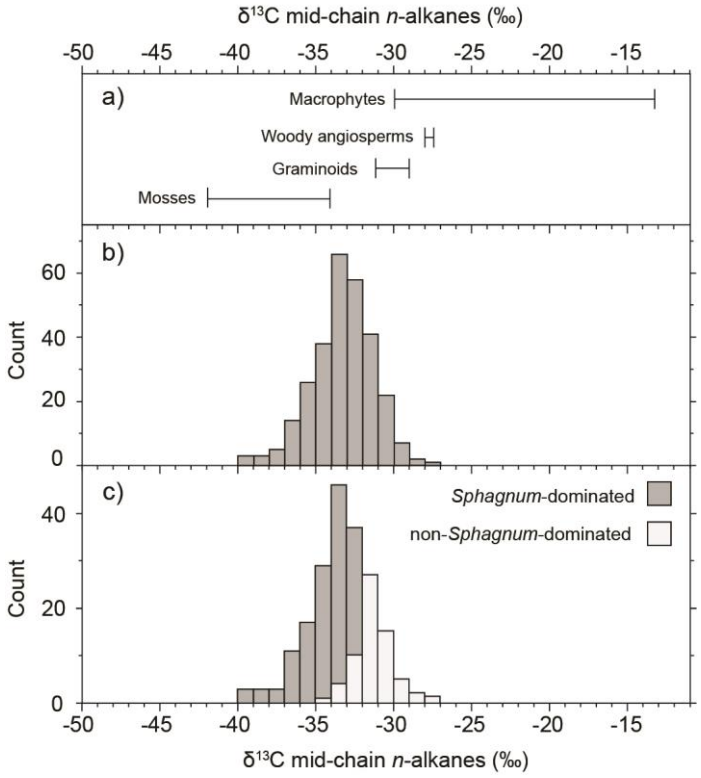

Figure 3: Compilation of mid-chain (C_{23}-C_{25}) *n*-alkane $\delta^{13}C$ values in (a) modern peatland plants (Aichner et al., 2010; Brader et al., 2010; Ficken et al., 1998; Huang et al., 2010; Huang et al., 2012; Mead et al., 2005; van Winden et al., 2010; Xie et al., 2004a), (b) *Sphagnum*-dominated peatlands *(this study*), and c) non-*Sphagnum* dominated peatlands (*this study*). Peatland *n*-alkane $\delta^{13}C$ values reported from the upper 100 cm only.

Diploptene $\delta^{13}C$ values average -33‰ and range from -29 to -45‰ (n = 66, σ = 3.8‰, skewness = - 1.3; Fig. 4). There is only a weak correlation between the $\delta^{13}C$ value of diploptene and those of C_{31} hopanes ($r = 0.05$), mid-chain *n*-alkanes ($r = 0.18$) and long-chain *n*-alkanes ($r = 0.17$) $\delta^{13}C$ values. Where present, other C_{27} to C_{30}

hopanoids (≤ C_{30} hopanoids, hereafter; Fig. 4) also have relatively ^{13}C-depleted values. This includes the C_{27} hopene (-29.5‰; n = 4; σ = 1.8), C_{27}-α hopane (-31.7‰; n = 11; σ = 0.95), C_{29}-βα hopane (-32.4‰; n =13; σ = 2.4), C_{29}-ββ hopane (-31.7‰; n = 10; σ = 1.7), C_{30}-ββ hopane (-27.7‰; n = 3; σ = 0.7) and two C_{30} hopenes with unknown structures (see Inglis et al,. 2018). The earlier eluting C_{30} hopene $\delta^{13}C$ has an average value of -26.8‰ (n = 52; σ = 2.3). The later eluting C_{30} hopene is relatively ^{13}C-depleted (-29.2‰; n = 59; σ = 1.7).

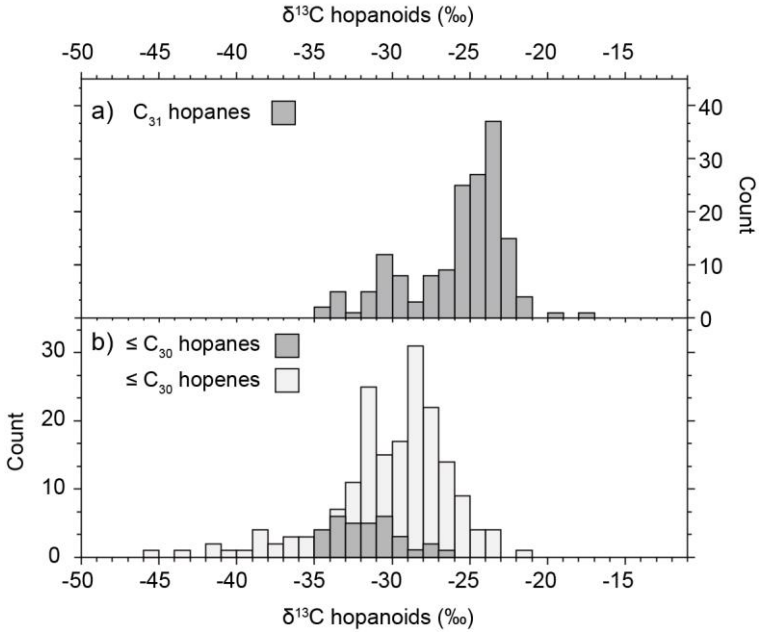

Figure 4: Compilation of hopanoid $\delta^{13}C$ values in recent peatlands. a) C_{31} hopane $\delta^{13}C$ values, and b) ≤ C_{30} hopanoid $\delta^{13}C$ values. The latter includes the following hopanoids: hop-22(29)-ene, C_{30} hopene(s), C_{27}-α hopane, C_{29}-βα hopane, C_{29}-ββ hopane and C_{30}-ββ hopane. Peatland hopanoid $\delta^{13}C$ values reported from the upper 100 cm only.

Within a single peatland, C_{31} hopanoids exhibit minor variations in $\delta^{13}C$ values (σ = 0.2 to 1.7‰; Fig. S1-S2) and the downcore variability (average σ = 1.2‰) is lower

than the global range (average σ = 2.6‰). There is no significant variation in C_{31} $\delta^{13}C$ values between deep and shallow sections of the peat (Fig. S1-S2). Although ≤ C_{30} hopanoid $\delta^{13}C$ values can exhibit more variation within a single peatland (e.g. Tibet; Fig. S2), the downcore variation (average σ: 2.1‰) remains lower than the global range (average σ = 3.7‰) with no significant variation in ≤ C_{30} hopanoid $\delta^{13}C$ values between deep (>15 cm) and shallow (<15 cm) sections of the peat (Fig. S1-S2).

4. Discussion

4.1 Photosynthetic pathway determines long-chain n-alkane $\delta^{13}C$ values

Within our dataset, long-chain (C_{29} to C_{33}) *n*-alkane $\delta^{13}C$ values exhibit a unimodal distribution and range between -29 and -37‰ (Fig. 2). This is consistent with previous studies in peatlands (Xie et al., 2004) and suggests that plants with the C_3 carbon fixation pathway dominated in the peat samples. However, long-chain *n*-alkane $\delta^{13}C$ values can also be influenced by a range of secondary environmental (e.g. $\delta^{13}C_{CO2}$, temperature, moisture content, altitude) and biosynthetic (e.g. plant functional type; PFT) controls (Diefendorf and Freimuth, 2017).

As peatlands are mostly water saturated, the influence of moisture content is likely to be relatively minor. However, moisture content can exert an indirect control on peatland vegetation and PFT. Here, we show that long-chain *n*-alkane $\delta^{13}C$ values in recent peatlands (-29 to -37‰; Fig. 2b) are comparable to *n*-alkanes extracted from key wetland plants (-29 to -36‰; Fig. 2a). This implies that changes in PFT are unlikely to significantly influence long-chain *n*-alkane $\delta^{13}C$ values. The only exception are aquatic macrophytes which can be significantly ^{13}C-enriched (Fig. 2a). However, we observe little evidence for macrophyte input in our peatland dataset (Fig. 2b; Supplementary Information).

Within our recent peatland dataset, long-chain *n*-alkane $\delta^{13}C$ values are linearly correlated with MAAT ($0.12 < R^2 < 0.39$). However, we argue that our relationship is partly driven by changes in the $\delta^{13}C$ composition of ambient CO_2 in the plant's immediate growth environment (i.e. the "canopy effect", characterised by a decrease in the $\delta^{13}C$ of plant biomass from the canopy to the forest floor) (Kohn, 2010). Confirming this, it is the samples from ^{13}C-depleted closed-canopy tropical forests (e.g. Peru, Indonesia) that dictate the relationship between long-chain *n*-alkane $\delta^{13}C$ values and MAAT in our dataset, and the correlation is negligible when these are removed ($R^2 < 0.1$). Altitude may also exert a control on *n*-alkane $\delta^{13}C$ values, with more ^{13}C-enriched values expected at higher altitude (Wu et al., 2017). However, due to the relatively large intra-site (up to 4‰) and inter-site variability (up to 10‰), long-chain *n*-alkane $\delta^{13}C$ values are poorly correlated with altitude in our dataset ($R^2 < 0.02$).

4.2 Aerobic methanotrophy influences mid-chain n-alkane $\delta^{13}C$ values

Within our recent peatland dataset, the weak correlation between mid-chain (C_{23} and C_{25}) and long-chain (C_{29} to C_{33}) *n*-alkane $\delta^{13}C$ values ($r = 0.07$ to 0.29) implies that mid-chain *n*-alkanes and long-chain *n*-alkanes are derived from different plant species. Indeed, within *Sphagnum*-dominated peatlands, mid-chain *n*-alkane $\delta^{13}C$ values range from -30 to -37‰ (Fig. 3b) and are ^{13}C-depleted (up to 5‰) relative to co-occurring long-chain *n*-alkanes. In contrast, mid-chain *n*-alkane $\delta^{13}C$ values within graminoid- and woody angiosperm-dominated peatlands range between -28 and 34‰ (Fig. 3b) and up to 6‰ enriched relative to co-occurring long-chain *n*-alkanes. Crucially, mid-chain *n*-alkane $\delta^{13}C$ values from *Sphagnum*- and non-*Sphagnum*-dominated peatlands are statistically different ($p < 0.01$). Taken together, this indicates preferential incorporation of ^{13}C-depleted CO_2 into mid-chain *n*-alkanes within

342 *Sphagnum*-dominated peatlands and provides evidence that *Sphagnum*-associated
343 methanotrophy is widespread (Kip et al., 2010; Raghoebarsing et al., 2005).

344 To explore changes in *Sphagnum*-associated methanotrophy, we calculated
345 $\Delta^{13}C_{alk}$ values (=$\bar{x}(\delta^{13}C_{23\text{-}25})$ - $\bar{x}(\delta^{13}C_{29\text{-}31})$) using our peatland dataset (following
346 Yamamoto et al., 2010). We show that $\Delta^{13}C_{alk}$ values from within *Sphagnum*-
347 dominated peatlands are negative and average -2.1 ± 1.6‰ (n = 112), indicating the
348 incorporation of ^{13}C-depleted carbon into mid-chain *n*-alkanes. This is consistent with
349 Elvert et al (2016) who report negative $\Delta^{13}C_{alk}$ values (-1.6 ± 0.7‰; n = 10) in a
350 thermokarst lake environment dominated by brown mosses. In contrast, within woody
351 angiosperm- and graminoid-dominated peatlands, $\Delta^{13}C$ values are positive (+2.6
352 ±1.6‰ and +1.3 ±0.6‰, respectively), indicating the absence of methanotrophy and/or
353 partially sub-aqueous growth (Ficken et al., 2000). To explore whether this offset is
354 mediated by other environmental controls, we examined the impact of temperature,
355 pH and altitude upon $\Delta^{13}C_{alk}$ values. Our results indicate that MAAT ($R^2 < 0.01$), pH
356 ($R^2 < 0.01$) and altitude ($R^2 = 0.02$) do not exert an important control on mid-chain *n*-
357 alkane $\delta^{13}C$ values. Instead, it is likely that water table level - via its influence on
358 *Sphagnum*-associated methanotrophy and carbon dioxide availability (e.g. Kip et al.,
359 2010; Raghoebarsing et al., 2005) - exerts an important control on $\Delta^{13}C_{alk}$ values.
360 Waterlogged conditions have been shown to enhance the activity of symbiotic
361 methanotrophs (Kip et al., 2010) and we suggest that a high water table will be
362 associated with the most negative $\Delta^{13}C_{alk}$ values. However, we note that excessively
363 waterlogged conditions can partially reduce CO_2 availability and will yield positive
364 $\Delta^{13}C_{alk}$ values (Brader et al., 2010; van Winden et al., 2010). The geological record
365 provides support for this observation with positive $\Delta^{13}C_{alk}$ values reported from an early
366 Eocene, waterlogged, *Sphagnum*-dominated bog (Inglis et al., 2015).

4.3. Heterotrophy is the primary control upon the $\delta^{13}C$ value of C_{31} hopanoid-producing bacteria

C_{31} hopanoids derive from a vast variety of bacteriohopanepolyols (BHPs), which in turn derive from diverse bacteria of highly variable ecology (Rohmer et al., 1984; Talbot and Farrimond, 2007). Despite this, previous studies in peatlands indicate that C_{31} hopanoid $\delta^{13}C$ values have a narrow range from -22 to -32‰ and are typically ^{13}C-enriched relative to bulk organic matter (e.g. Xie et al., 2004; Pancost et al., 2000; Pancost et al., 2003). In our dataset, $\delta^{13}C$ values of C_{31} hopanoids range between -20 and -35‰ (Fig. 4a), expanding the known range as might be expected for a compound with such diverse sources. $\delta^{13}C$ values of C_{31} hopane stereoisomers (i.e. ββ and αβ) are positively correlated (r = 0.87), indicating they are likely derived from the same bacterial source. Intriguingly, the observation that C_{31} hopanoid $\delta^{13}C$ values are ^{13}C-enriched relative to co-occurring leaf wax biomarkers (long-chain *n*-alkanes) is universally retained, despite the significant variety of precursor compounds and organisms (see Talbot et al., 2016a and ref. therein). This supports previous suggestions (Pancost et al., 2003), based on limited data, that C_{31} hopanoids are derived from heterotrophic bacteria consuming ^{13}C-enriched substrates (e.g. carbohydrates) and confirms that organic substrate exerts an important control on C_{31} hopane $\delta^{13}C$ values. We note that the magnitude of this offset is not constant, ranging from 0 to 10‰ (Fig. S3) and likely records varying degrees of substrate preference.

These interpretations are supported by the dominance of bacteriohopanetetrol (BHT) and BHT cyclitol ether in recent peatlands (Kim et al., 2011; van Winden et al., 2012; Talbot et al., 2016a; Fig. S4). Multiple heterotrophic (but also other) sources are expected for both compounds. However, most heterotrophs synthesise BHT whilst BHT cyclitol ether is the most commonly occurring BHP in members of the Alpha-,

393 Beta-, Gamma and Deltaproteobacteria (e.g. *Burkholderia*, *Bradyrhizobium*,
394 *Rhodoblastus*, as well as other phyla including the Cyanobacteria, Acidobacteria and
395 Acetobacteria; Talbot et al., 2016a). A largely heterotrophic bacterial community is
396 also consistent with the low abundance of BHPs assigned to methane oxidising
397 bacteria (35-aminobacteriohopanepentol and 35-aminobacteriohopanetetrol). Taken
398 together, this suggests that the majority of hopanoid-producing bacteria in peatlands
399 are heterotrophs. It is unclear what the $\delta^{13}C$ signature of autotroph-derived hopanoids
400 would be; however, given the discrimination between biomass and CO_2 substrate
401 during autotrophy (Pancost and Sinninghe Damsté, 2003 and ref. therein), it is
402 expected to be somewhat depleted relative to the associated sedimentary organic
403 matter.

404 Using our recent dataset, we examined the impact of temperature, pH and
405 altitude upon the $\delta^{13}C$ value of C_{31} hopanoid-producing bacteria. There is a weak
406 correlation between C_{31} hopane $\delta^{13}C$ values and pH ($R^2 = 0.09$) and altitude ($R^2 <$
407 0.01). There is a linear correlation between C_{31} hopanoid $\delta^{13}C$ values and MAAT (R^2
408 = 0.68), with lower values occurring in tropical settings. However, C_{31} hopanoid $\delta^{13}C$
409 values are also significantly correlated with C_{29}, C_{31} and C_{33} *n*-alkane $\delta^{13}C$ values (r =
410 0.37, 0.71 and 0.62 respectively) and we argue that this relationship is partly driven
411 by the aforementioned controls on plant $\delta^{13}C$ (i.e. the "canopy effect"; see 4.1). This
412 agrees with previous studies which document a close relationship between bulk
413 organic matter, long-chain *n*-alkane and C_{31} hopane $\delta^{13}C$ values in peatland
414 environments (e.g. Pancost et al., 2003). Collectively, this implies that C_{31} hopanoids
415 are unsuitable, low-sensitivity candidates for tracing modern and past changes in the
416 CH_4 cycle (but see below).

417

4.4. Methanotrophy and heterotrophy exert a control on the $\delta^{13}C$ value of ≤ C_{30} hopanoid-producing bacteria

In our dataset, C_{27} to C_{30} hopanoids (i.e. ≤ C_{30} hopanoids, including αβ, βα and ββ stereoisomers) exhibit a larger range and have lower values compared to the C_{31} hopanoids (Fig. 4b). In most settings, ≤ C_{30} hopanoid $\delta^{13}C$ values range between -28 and -35‰, suggesting that they are derived from a largely heterotrophic bacterial community. This is consistent with the dominance of saturated tetrafunctionalised BHPs (e.g. BHT, BHT cyclitol ether, aminotriol) in two of the peatlands studied here (Bissendorfer Moor, Germany, and Misten Bog, Belgium; Fig. S4) and the interpretation of C_{31} hopanoid $\delta^{13}C$ values. However, ≤ C_{30} hopanoids $\delta^{13}C$ values are always lower than those of the corresponding C_{31} hopanoids, suggesting a minor methanotroph contribution.

Crucially, in some settings, ≤ C_{30} hopanoids are strongly ^{13}C-depleted (up to -45‰; Fig. 4b) and are up to 15‰ more negative than relative to co-occurring long-chain *n*-alkanes and C_{31} hopanes. In the context of peatlands, it is therefore clear that ≤ C_{30} hopanoids can be derived from a mixed bacterial population consuming plant biomass but also more ^{13}C-depleted carbon (e.g. recycled CO_2 and/or CH_4). This indicates a strong source decoupling between ≤ C_{30} and C_{31} hopanoids. Previous analyses of Eocene-aged lacustrine sediments have suggested such decoupling (Freeman et al., 1990; Volkman et al., 2015), as have analyses of modern cyanobacterial mats and cultures (Jahnke et al., 1999; Summons et al., 1994). Our work suggests a more profound and widespread decoupling in peatlands that has significant implications for future hopanoid $\delta^{13}C$ interpretation.

Carbon isotopic decoupling is not expected but is consistent with and can be attributed to the different sources of ≤ C_{30} and C_{31} hopanoids. C_{31} hopanoids are derived exclusively from oxidation and decarboxylation of saturated

444 tetrafunctionalised BHPs (Inglis et al., 2018 and ref. therein). Multiple bacterial sources
445 are expected for these compounds; however, heterotrophs are the most likely source
446 in peatlands (Talbot et al., 2016a). In contrast, C_{27} to C_{30} hopanoids can be derived
447 from a more diverse suite of precursor compounds (e.g. penta- and hexafuntionalised
448 BHPs, diplopterol, diploptene; Talbot and Farrimond, 2007; Talbot et al., 2014). These
449 compounds can be derived from a wider range of source bacteria (including
450 methanotrophs) and provides an explanation for why ≤ C_{30} hopanoids have more
451 negative $\delta^{13}C$ values and are the more sensitive recorder of terrestrial CH_4 cycling (c.f.
452 C_{31} hopanes). By extension, the sources of C_{31} hopanes means they likely have limited
453 utility as a methanotroph biomarker in such settings, both in terms of distributions and
454 isotopic composition, revealing why previous BHP analyses in peat (Talbot et al.,
455 2016a) and lignite deposits (Talbot et al., 2016b) failed to detect a strong
456 methanotroph signal.
457
458 ***4.5. Influence of environmental processes on the $\delta^{13}C$ value of ≤ C_{30} hopanoid***
459 ***producing bacteria***
460
461 Using our global dataset, we also examined the impact of temperature, pH and altitude
462 upon the $\delta^{13}C$ value of ≤ C_{30} hopanoid-producing bacteria. Previous studies indicate
463 that CH_4 oxidation rates and temperature are closely coupled (Dunfield et al., 1993;
464 Segers, 1998; van Winden et al., 2012a). This implies that ≤ C_{30} hopanoid $\delta^{13}C$ values
465 and temperature will be related, as found by Elvert et al. (2016). A close
466 correspondence between $\delta^{13}C$ values and temperature was previously observed
467 within a mesocosm study, with lower $\delta^{13}C$ values (indicating greater incorporation of
468 CH_4) at higher temperatures (van Winden et al., 2011). However, there is only a weak
469 relationship between ≤ C_{30} hopanoid $\delta^{13}C$ values and temperature (R^2 = 0.02) in our

dataset (Fig. S5) and recent studies have argued that substrate availability (rather than temperature) is the primary control upon CH_4 oxidation rates (Lofton et al., 2014; Megonigal and Schlesinger, 2002; Yvon-Durocher et al., 2014).

To explore other potential environmental drivers, we compared ≤ C_{30} hopanoid $\delta^{13}C$ values alongside key environmental parameters (including altitude, pH and vegetation). Our results indicate that altitude does not exert a strong control and there is only a weak relationship between ≤ C_{30} hopanoid $\delta^{13}C$ values and altitude (R^2 = 0.22). Instead, low ≤ C_{30} hopanoid $\delta^{13}C$ values are closely related to measured pH and the lowest ≤ C_{30} hopanoid $\delta^{13}C$ values occur in peatlands with pH 5 to 6.5 (Fig. S5). This is the optimum pH for peatland methanogenesis (Kotsyurbenko et al. 2004) and suggests that low ≤ C_{30} hopanoid $\delta^{13}C$ values reflect an increase in CH_4 availability to the source bacteria.

It is also likely that a range of other factors will exert a control upon the $\delta^{13}C$ value of ≤ C_{30} hopanoid-producing bacteria in peatlands. Local hydrology could exert an indirect control because minerotrophic (i.e. rainwater and groundwater-fed) fens are characterised by higher CH_4 emissions compared to ombrotrophic (i.e. rainwater-fed) bogs (Moore and Knowles, 1990; Turetsky et al., 2014). This is consistent with the occurrence of the lowest ≤ C_{30} hopanoid $\delta^{13}C$ values in minerotrophic fens, including Huanyuan, China (up to -44‰), Tamiami Sawgrass, USA (-38‰), Buena Vista del Maquia, Peru (up to -45‰) and Tacshacocha, Peru (-39 ‰). Vegetation can also exert an indirect control on methanotrophy because non-woody vascular plants (e.g. sedges) can transport oxygen from the atmosphere to the rhizosphere, helping to promote CH_4 oxidation at depth (King et al., 1998; Zheng et al., 2014). This is consistent with low ≤ C_{30} hopanoid $\delta^{13}C$ values in graminoid-dominated peatlands, including Huanyuan, China (up to -44‰) and Tamiami Sawgrass, USA (-38‰).

However, vegetation can also act as a conduit for CH_4 release, thereby reducing the probability of CH_4 oxidation (Schuldt et al., 2013).

Differences in methanotroph assimilation pathways may also exert an indirect control upon hopanoid $\delta^{13}C$ values. For example, methanotrophs using the ribulose monophosphate pathway (i.e. Type I methanotrophs) typically exhibit much more depleted $\delta^{13}C$ lipid values than methanotrophs using the serine pathway (i.e. Type II methanotrophs). The absence of very low (< -60‰) $\delta^{13}C$ lipid values in our dataset suggests that Type II methanotrophs dominate. This is consistent with microbiological studies (e.g. Dedysh et al., 2001; 2009; Kip et al., 2011) and the low abundance of aminopentol (a biomarker for Type I methanotrophs) in most peatlands (e.g. Talbot et al., 2016a). Finally, the $\delta^{13}C$ value of CH_4 will also influence ≤ C_{30} hopanoid $\delta^{13}C$ values; for example, CH_4 produced in ombrotrophic peatlands has a $\delta^{13}C$ composition that is significantly more negative than that of CH_4 formed in fens (Hornibrook and Bowes, 2007). However, the lowest $\delta^{13}C$ lipid values in our study are associated with fen environments, confirming that low ≤ C_{30} hopanoid $\delta^{13}C$ values, at least in this reference set, primarily reflect an increase in CH_4 availability to the source bacteria (rather than changes in its isotopic composition).

Collectively, our dataset indicates that ≤ C_{30} hopanoid $\delta^{13}C$ values are influenced by a range of environmental (e.g. pH, vegetation, trophic status) and biological variables (e.g. diverse biohopanoid precursors and ecologies of source bacteria). Given that, it is remarkable that isotopic relationships are consistent over a wide range of ecologically and climatically diverse sites. The ≤ C_{30} hopanoids are always depleted relative to co-occurring C_{31} hopanoids and are depleted relative to plant biomarkers only in settings with elevated, near neutral pH with inferred relatively high rates of methanogenesis. Such complexity of environmental and biological controls probably

explains the lack of other clear relationships, i.e. with temperature; this could be explored by future targeted studies that include microbiological characterisation. Nonetheless, the occurrence of ^{13}C-depleted ≤ C_{30} hopanoids (up to -45‰) in peatlands provides clear evidence for the incorporation of isotopically light CH_4 into the bacterial community and confirms that ≤ C_{30} hopanoids have potential for qualitatively tracking changes in peatland CH_4 cycling.

4.6. Re-evaluating methane cycling in the geological record

Here we revisit previously published hopanoid $\delta^{13}C$ records in (fossilised) peat archives from: 1) the early-to-middle Holocene and late Glacial (4 to 18 thousand years ago; Zheng et al., 2014; Elvert et al., 2016; Huang et al., 2018), and 2) the early Eocene and latest Paleocene (48 to 56 million years ago; Pancost et al., 2007; Inglis et al., 2015). Here we adopt an approach based on coupled hopanoid-leaf wax $\delta^{13}C$ values because it is evident, especially for the C_{31} hopanoids, that hopanoid $\delta^{13}C$ values are partly governed by those of associated plant matter. To provide a baseline for interpreting past variations in the CH_4 cycle, we calculate $\Delta^{13}C_{hop\text{-}alk}$ values (= $\delta^{13}C_{hopanoid}$ - $\delta^{13}C_{alkane}$). This removes the impact of vegetation upon hopanoid $\delta^{13}C$ values (e.g. the “canopy effect”). Note that we have normalised hopanoid values to the C_{29} *n*-alkane (Fig. 5); however, similar results are obtained when other long-chain *n*-alkanes are used (i.e. C_{31} and C_{33}). This approach: 1) draws an even sharper contrast between the isotopic behaviour of ≤ C_{30} hopanoids and C_{31} hopanoids (Fig. 5); and 2) reveals that $\Delta^{13}C_{hop\text{-}alk}$ values below -10‰ are indicative of more intense aerobic methanotrophy than observed in our recent peatland dataset. Crucially, as methanotrophy and methanogenesis can be tightly coupled in modern peatlands (van Winden et al., 2012a), low $\Delta^{13}C_{hop\text{-}alk}$ values can be interpreted as evidence for an

545 invigorated CH_4 cycle. Importantly, this approach can be used to re-interpret published
546 hopanoid $\delta^{13}C$ data from (fossilised) peat archives, especially where *n*-alkane $\delta^{13}C$
547 values had been published or could be obtained for this study (Figure 6).

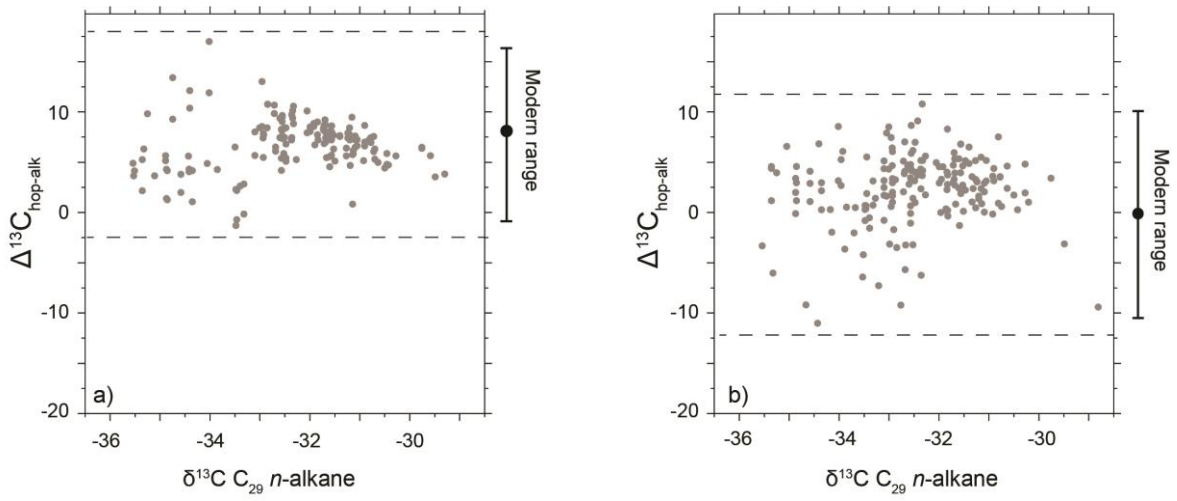

Figure 5: Compilation of $\Delta^{13}C_{hop\text{-}alk}$ values (= $\delta^{13}C_{hopanoid}$ - $\delta^{13}C_{alkane}$) in recent peatlands. a) C_{31} hopanoid $\delta^{13}C$ values normalised to C_{29} *n*-alkane $\delta^{13}C$ value, and b) ≤ C_{30} hopanoid $\delta^{13}C$ values normalised to C_{29} *n*-alkane $\delta^{13}C$ value. Values which are negative and fall outside the modern range provide evidence for enhanced methane cycling relative to the 'recent' peatland dataset.

548

549 ***4.6.1. Mid-to-Early Holocene and latest Glacial (4 to 18 ka)***

550 Here, we revisit published $\delta^{13}C_{lipid}$ values from peat archives spanning the middle-to-
551 early Holocene and last glacial termination (ca. 4 to 18 thousand years ago; ka). These
552 peats are located in eastern China (ca. 4 to 13 ka; Zheng et al., 2014), central China
553 (ca. 4 to 18 ka; Huang et al, 2018) and Alaska (ca. 4 to 12 ka; Elvert et al., 2016). It is
554 evident from these published studies that ≤ C_{30} hopanoids can be ^{13}C-depleted and
555 $\Delta^{13}C_{hop\text{-}alk}$ values low within late Glacial and mid-to-early Holocene peat archives
556 (Zheng et al., 2014; Elvert et al., 2016; Huang et al., 2018; Fig. 6b) For example, low
557 ≤ C_{30} hopanoid $\delta^{13}C$ values (up to -40‰) and low $\Delta^{13}C_{hop\text{-}alk}$ values (up to -8‰) are

558 reported from central China during the mid-Holocene (~5 to 8 ka; Huang et al., 2018).
559 In exceptional circumstances, these values can be far lower than in our recent dataset.
560 In southwest China, ≤ C_{30} hopanoid $\delta^{13}C$ values decrease to -50‰ (Zheng et al., 2014)
561 and $\Delta^{13}C_{hop\text{-}alk}$ values decrease to -17‰ during the middle Holocene (~5 ka). Low ≤
562 C_{30} hopanoid $\delta^{13}C$ values (as low as -55‰) and low $\Delta^{13}C_{hop\text{-}alk}$ values (as low as -
563 26‰) are also reported from an Alaskan peat during the early Holocene (~10 to 12 ka;
564 Elvert et al., 2016). In both cases, these light values were previously interpreted as
565 evidence for an enhanced CH_4 cycle. However, because absolute values and $\Delta^{13}C_{hop\text{-}}$
566 $_{alk}$ values are well below the modern range, they can now be interpreted as evidence
567 for enhanced CH_4 cycling. In contrast, C_{31} hopanoid $\delta^{13}C$ values in mid-to-early
568 Holocene samples typically range between -22 and -30‰ (Fig. 6). This is consistent
569 with our "recent" peatland dataset and emphasises the differing isotopic behaviour of
570 ≤ C_{30} and C_{31} hopanoids in natural settings. However, there are exceptions (see 4.6.2
571 below).

572 Our "recent" peatland dataset also helps us to understand the mechanistic link
573 between past climate change and CH_4 cycle perturbations. In particular, the
574 association of ^{13}C-depleted hopanoids in recent peats with relatively high pH (5 to 6)
575 – and the hydrological and ecological conditions that yield such pH conditions –
576 appears to also explain past records. For example, during the early Holocene, low
577 hopanoid $\delta^{13}C$ values in Alaska coincide with more negative long-chain *n*-alkane $\delta^{2}H$
578 values (Elvert et al., 2016), suggesting enhanced moisture transport and a microbial
579 response to wetter conditions. Intriguingly, the opposite is observed during the mid-
580 Holocene in central China, where low hopanoid $\delta^{13}C$ values coincide with inferred
581 dryer (but variable) conditions and near neutral pH (pH 5 to 6) (Huang et al., 2018).
582 Inferred dry conditions and near neutral pH values (pH 5 to 6) are also associated

583 with low hopanoid $\delta^{13}C$ values in eastern China during the mid-Holocene (Zheng et
584 al., 2014). Within eastern China, low values hopanoid $\delta^{13}C$ values coincide with a
585 decrease in methanogen biomass (Zheng et al., 2014). This is somewhat counter-
586 intuitive and therefore suggests a change in CH_4 flux pathways at a time where overall
587 CH_4 production was lower and the region experienced a sustained drying event
588 (Chen et al., 2006; Zhao et al., 2007). Thus, in this setting, decreased
589 methanogenesis is attributed to drier and more oxidising conditions caused by
590 weakening of the Asian summer monsoon, and increased methanotrophy is
591 attributed to the development of longer and thicker sedge roots and more diffusive
592 CH_4 flux as the water table deepened. Collectively, this demonstrates the complexity
593 of the terrestrial CH_4 cycle and its sensitivity to hydrological perturbations, especially
594 as a transient response to climate change (e.g. drying/rewetting cycles; Knorr et al.,
595 2008; Mitsch et al., 2010; Turetsky et al., 2014).
596

597 ***4.6.2. Latest Paleocene and early Eocene (48 to 56 Ma)***

598 We also revisit published $\delta^{13}C$ values from fossilised peat archives (lignites) spanning
599 the latest Paleocene and early Eocene (56 to 48 Ma). These peats were deposited in
600 the UK (Pancost et al., 2007) and Germany (Inglis et al., 2015). The lowest reported
601 $\delta^{13}C$ values (-75‰) and $\Delta^{13}C$ values (-46‰) are observed within the UK during the
602 onset of the Paleocene-Eocene Thermal Maximum (PETM; 56 Ma; Pancost et al.,
603 2007). These values are significantly lower than those obtained from the Holocene
604 and indicate a particularly exceptional response of the CH_4 cycle. The Paleocene-
605 Eocene Thermal Maximum is also associated with the unusual occurrence of low C_{31}
606 hopanoid $\delta^{13}C$ values (as low as -47‰; Pancost et al., 2007) and low $\Delta^{13}C_{hop\text{-}alk}$ values
607 (as low as -19‰) (Fig. S6). Crucially, both coincide with an increase in the occurrence

608 of bacteriohopanepolyols assigned directly to methanotrophic bacteria (Talbot et al.,
609 2016a).

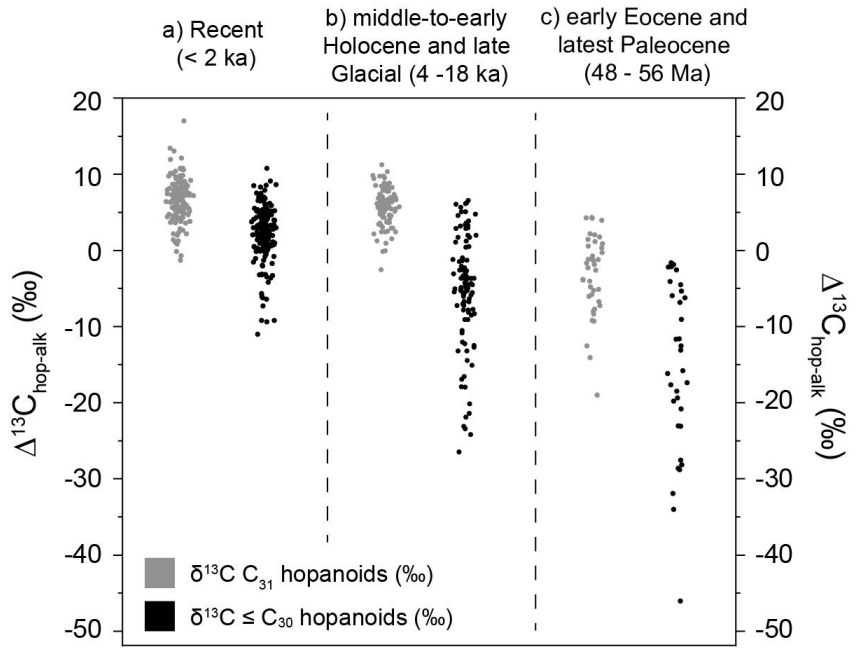

Figure 6: Compilation of $\Delta^{13}C_{hop\text{-}alk}$ values in: a) recent peatlands (*this study*), b) middle-to-early Holocene and late Glacial peat archives (4 to 18 ka) (Elvert et al., 2016; Huang et al., 2018; Zheng et al., 2014; n = 108), and c) early Eocene and latest Paleocene lignites (48 to 56 Ma) (Inglis et al., 2015; Pancost et al., 2007; n = 59).

610

611 During the Paleocene-Eocene Thermal Maximum (Pancost et al., 2007), low ≤
612 C_{30} and C_{31} hopanoid $\delta^{13}C$ values coincide with the onset of waterlogged conditions
613 and a shift in reconstructed pH towards near neutral values (Fig. S6). The PETM is
614 also associated with an increase in 35-aminobacteriohopanepentol (aminopentol),
615 indicating an increase in Type I methanotrophic bacteria (i.e. Gammaproteobacteria).
616 As Type I methanotrophs typically exhibit much more depleted $\delta^{13}C$ lipid values, this
617 likely explains why we observe low $\delta^{13}C$ values and $\Delta^{13}C_{hop\text{-}alk}$ values within both the

618 ≤C_{30} and C_{31} hopanoids. Although there have been few subsequent investigations on
619 peatland CH_4 cycling during the PETM, early Eocene and late Paleocene peatlands
620 were far more extensive than today (up to ~3 times greater) and modelled CH_4
621 emissions far exceed those for the modern pre-industrial world (Beerling et al., 2011).
622 As CH_4 is a potent greenhouse gas, enhanced peatland methane emissions could
623 have helped to amplify warming to a greater degree than estimated using existing
624 model simulations and should be incorporated into future studies.

625 Taken together, this highlights the importance of pH, hydrology and ecology
626 (rather than temperature; see Pancost et al., 2007) in regulating hopanoid $\delta^{13}C$ values
627 in peatland environments, including during episodes of environmental change. Future
628 work tracing past changes in the CH_4 cycle, therefore, would benefit from
629 accompanying proxy-based pH and hydrological reconstructions based on, for
630 example, the distribution of hopanes (Inglis et al., 2018) or branched glycerol dialkyl
631 glycerol tetraethers (brGDGTs) (Naafs et al., 2017) and the hydrogen isotope
632 composition of leaf wax biomarkers (Sachse et al., 2012)

633

634 ***5. Conclusions***

635 Using samples from peatlands from different geographic regions we demonstrate the
636 incorporation of ^{13}C-depleted CO_2 and/or CH_4 into mid-chain *n*-alkanes and ≤ C_{30}
637 hopanoids. Our results confirm that both are suitable candidates for tracking changes in
638 peatland CH_4 cycling. Re-analysis of published data from the mid-to-early Holocene and
639 late Glacial (4 to 18 ka) and early Eocene and latest Paleocene (48 to 56 Ma) indicates
640 that ≤ C_{30} hopanoids can be extremely ^{13}C-depleted within both peat archives and lignite
641 deposits (up to -75‰). Such values are well below the recent (<2 ka) range and can now
642 be interpreted as particularly exceptional responses of the methane cycle to past climate

perturbations. These results indicate that lipid biomarkers are important tools for evaluating modern and ancient biogeochemical processes and could potentially provide insights into terrestrial CH_4 cycling over the Cenozoic and Mesozoic.

Acknowledgements

This research was funded through the advanced ERC grant 'The Greenhouse Earth System' (T-GRES. Project reference: 340923). RDP acknowledges the Royal Society Wolfson Research Merit Award. BDAN also received funding through a Royal Society Tata University Research Fellowship. YZ acknowledges the National Natural Science Foundation of China Grants (41872031). GNI thanks X. Huang, S. Yamamoto, J. van Winden for providing raw data and J. Blewett, K. Freeman R.P. Evershed for useful discussions. We also thank the NERC Life Sciences Mass Spectrometry Facility (Bristol) for analytical support and D. Atkinson for help with the sample preparation. Members of the T-GRES Peat Database collaborators are M.J. Amesbury, H. Biester, R. Bindler, J. Blewett, M.A. Burrows, D. del Castillo Torres, F.M. Chambers, A.D. Cohen, S.J. Feakins, M. Gałka, A. Gallego-Sala, L. Gandois, D.M. Gray, P.G. Hatcher, E.N. Honorio Coronado, P.D.M. Hughes, A. Huguet, M. Könönen, F. Laggoun-Défarge, O. Lähteenoja, M. Lamentowicz, R. Marchant, X. Pontevedra-Pombal, C. Ponton, A. Pourmand, A.M. Rizzuti, L. Rochefort, J. Schellekens, F. De Vleeschouwer. Finally, we thank Ed Hornibrook, Sabine Kasten, Marcus Elvert and two anonymous reviewers whose thoughtful comments significantly improved the manuscript.

References

667 Aaby, B. and Tauber, H. (1975) Rates of peat formation in relation to degree of
668 humification and local environment, as shown by studies of a raised bog in
669 Deninark. *Boreas* **4**, 1-17.

670 Aichner, B., Wilkes, H., Herzschuh, U., Mischke, S. and Zhang, C. (2010) Biomarker
671 and compound-specific $\delta^{13}C$ evidence for changing environmental conditions
672 and carbon limitation at Lake Koucha, eastern Tibetan Plateau. *Journal of*
673 *Paleolimnology* **43**, 873-899.

674 Beerling, D.J., Fox, A., Stevenson, D.S. and Valdes, P.J. (2011) Enhanced chemistry-
675 climate feedbacks in past greenhouse worlds. *Proceedings of the National*
676 *Academy of Sciences*. **108**. 9770-9775

677 Brader, A.V., van Winden, J.F., Bohncke, S.J., Beets, C.J., Reichart, G.-J. and de
678 Leeuw, J.W. (2010) Fractionation of hydrogen, oxygen and carbon isotopes in *n*-
679 alkanes and cellulose of three *Sphagnum* species. *Organic Geochemistry* **41**,
680 1277-1284.

681 Bridgham, S.D., Cadillo-Quiroz, H., Keller, J.K. and Zhuang, Q. (2013) Methane
682 emissions from wetlands: biogeochemical, microbial, and modeling perspectives
683 from local to global scales. *Global Change Biology* **19**, 1325-1346.

684 Broder, T. and Biester, H.(2015) Hydrologic controls on DOC, As and Pb export from
685 a polluted peatland–the importance of heavy rain events, antecedent moisture
686 conditions and hydrological connectivity. *Biogeosciences*. **12**, 4651-4664.

687 Chambers, F.M., Brain, S.A., Mauquoy, D., McCarroll, J. and Daley, T.J.T.H. (2014)
688 The 'Little Ice Age'in the Southern Hemisphere in the context of the last 3000
689 years: Peat-based proxy-climate data from Tierra del Fuego. *The Holocene.* **24**,
690 1649-1656.

691 Chen, F.-H., Cheng, B., Zhao, Y., Zhu, Y. and Madsen, D.B. (2006) Holocene
692 environmental change inferred from a high-resolution pollen record, Lake
693 Zhuyeze, arid China. *The Holocene.* **16**, 675-684.
694 Collister, J.W., Rieley, G., Stern, B., Eglinton, G. and Fry, B. (1994) Compound-
695 specific $\delta^{13}C$ analyses of leaf lipids from plants with differing carbon dioxide
696 metabolisms. *Organic Geochemistry* **21**, 619-627.
697 Davies, K., Pancost, R., Edwards, M., Walter Anthony, K., Langdon, P. and Chaves
698 Torres, L. (2015) Diploptene $\delta^{13}C$ values from contemporary thermokarst lake
699 sediments show complex spatial variation. *Biogeosciences.* **13**, 2611-2621.
700 De Vleeschouwer, F., Pazdur, A., Luthers, C., Streel, M., Mauquoy, D., Wastiaux, C.,
701 Le Roux, G., Moschen, R., Blaauw, M. and Pawlyta, J., Sikorski, J., Piotrowska,
702 N (2012) A millennial record of environmental change in peat deposits from the
703 Misten bog (East Belgium). *Quaternary International*. **268**, 44-57.
704 Dean, J.F., Middelburg, J.J., Röckmann, T., Aerts, R., Blauw, L.G., Egger, M., Jetten,
705 M.S., Jong, A.E., Meisel, O.H. and Rasigraf, O., Slomp, C.P in't Zandt, M.H. and
706 Dolman, A.J. (2018) Methane feedbacks to the global climate system in a warmer
707 world. *Reviews of Geophysics*, **56**, 207-250
708 Diefendorf, A.F., Freeman, K.H., Wing, S.L. and Graham, H.V. (2011) Production of
709 n-alkyl lipids in living plants and implications for the geologic past. *Geochimica*
710 *et Cosmochimica Acta* **75**, 7472-7485.
711 Diefendorf, A.F. and Freimuth, E.J. (2017) Extracting the most from terrestrial plant-
712 derived *n*-alkyl lipids and their carbon isotopes from the sedimentary record: A
713 review. *Organic Geochemistry* **103**, 1-21.

714 Dunfield, P., Dumont, R. and Moore, T.R. (1993) Methane production and
715 consumption in temperate and subarctic peat soils: response to temperature and
716 pH. *Soil Biology and Biochemistry* **25**, 321-326.
717 Elvert, M., Pohlman, J.W., Becker, K.W., Gaglioti, B., Hinrichs, K.-U. and Wooller, M.J.
718 (2016) Methane turnover and environmental change from Holocene lipid
719 biomarker records in a thermokarst lake in Arctic Alaska. *The Holocene.* **26**,
720 1766-1777.
721 Farquhar, G.D., Ehleringer, J.R. and Hubick, K.T. (1989) Carbon isotope
722 discrimination and photosynthesis. *Annual Review of Plant Biology* **40**, 503-537.
723 Ficken, K., Barber, K. and Eglinton, G. (1998) Lipid biomarker, $\delta^{13}C$ and plant
724 macrofossil stratigraphy of a Scottish montane peat bog over the last two
725 millennia. *Organic Geochemistry* **28**, 217-237.
726 Ficken, K., Li, B., Swain, D. and Eglinton, G. (2000) An *n*-alkane proxy for the
727 sedimentary input of submerged/floating freshwater aquatic macrophytes.
728 *Organic Geochemistry* **31**, 745-749.
729 Freeman, K.H., Hayes, J., Trendel, J.-M. and Albrecht, P. (1990) Evidence from
730 carbon isotope measurements for diverse origins of sedimentary hydrocarbons.
731 *Nature* **343**, 254.
732 Gorham, E. (1991) Northern peatlands: role in the carbon cycle and probable
733 responses to climatic warming. *Ecological Applications*. **1**, 182-195.
734 Hornibrook, E.R. and Bowes, H.L. (2007) Trophic status impacts both the magnitude
735 and stable carbon isotope composition of methane flux from peatlands.
736 Geophysical Research Letters. **34**. L21401

737 Huang, X., Pancost, R.D., Xue, J., Gu, Y., Evershed, R.P. and Xie, S. (2018)
738 Response of carbon cycle to drier conditions in the mid-Holocene in central
739 China. *Nature Communications* **9**, 1369.
740 Huang, X., Wang, C., Xue, J., Meyers, P.A., Zhang, Z., Tan, K., Zhang, Z. and Xie, S.
741 (2010) Occurrence of diploptene in moss species from the Dajiuhu Peatland in
742 southern China. *Organic Geochemistry* **41**, 321-324.
743 Huang, X., Xue, J., Zhang, J., Qin, Y., Meyers, P.A. and Wang, H. (2012) Effect of
744 different wetness conditions on *Sphagnum* lipid composition in the Erxianyan
745 peatland, central China. *Organic Geochemistry* **44**, 1-7.
746 Inglis, G.N., Collinson, M.E., Riegel, W., Wilde, V., Robson, B.E., Lenz, O.K. and
747 Pancost, R.D. (2015) Ecological and biogeochemical change in an early
748 Paleogene peat-forming environment: Linking biomarkers and palynology.
749 *Palaeogeography, Palaeoclimatology, Palaeoecology* **438**, 245-255.
750 Inglis, G.N., Naafs, B.D.A., Zheng, Y., McClymont, E.L., Evershed, R.P. and Pancost,
751 R.D. (2018) Distributions of geohopanoids in peat: Implications for the use of
752 hopanoid-based proxies in natural archives. *Geochimica et Cosmochimica Acta*
753 **224**, 249-261.
754 Jacob, J., Disnar, J.-R., Boussafir, M., Albuquerque, A.L.S., Sifeddine, A. and Turcq,
755 B. (2005) Pentacyclic triterpene methyl ethers in recent lacustrine sediments
756 (Lagoa do Caçó, Brazil). *Organic Geochemistry.* **36**, 449-461.
757 Jahnke, L.L., Summons, R.E., Hope, J.M. and Des Marais, D.J. (1999) Carbon isotopic
758 fractionation in lipids from methanotrophic bacteria II: The effects of physiology
759 and environmental parameters on the biosynthesis and isotopic signatures of
760 biomarkers. *Geochimica et Cosmochimica Acta* **63**, 79-93.

761 Jauhiainen, J., Takahashi, H., Heikkinen, J.E., Martikainen, P.J. and Vasander, H.
762 (2005) Carbon fluxes from a tropical peat swamp forest floor. *Global Change*
763 *Biology.* **11**, 1788-1797.
764 King, J.Y., Reeburgh, W.S. and Regli, S.K. (1998) Methane emission and transport by
765 arctic sedges in Alaska: results of a vegetation removal experiment. *Journal of*
766 *Geophysical Research: Atmospheres* **103**, 29083-29092.
767 Kip, N., van Winden, J.F., Pan, Y., Bodrossy, L., Reichart, G.-J., Smolders, A.J.P.,
768 Jetten, M.S.M., Damste, J.S.S. and Op den Camp, H.J.M. (2010) Global
769 prevalence of methane oxidation by symbiotic bacteria in peat-moss
770 ecosystems. *Nature Geoscience* **3**, 617-621.
771 Knorr, K.-H., Oosterwoud, M.R., Blodau, C. (2008) Experimental drought alters rates
772 of soil respiration and methanogenesis but not carbon exchange in soil of a
773 temperate fen. *Soil Biology and Biochemistry.* **40**, 1781-1791.
774 Kohn, M.J. (2010) Carbon isotope compositions of terrestrial C_3 plants as indicators of
775 (paleo) ecology and (paleo) climate. *Proceedings of the National Academy of*
776 *Sciences* **107**, 19691-19695.
777 Kotsyurbenko, O. R., Chin, K. J., Glagolev, M. V., Stubner, S., Simankova, M. V.,
778 Nozhevnikova, A. N., and Conrad, R (2004) Acetoclastic and hydrogenotrophic
779 methane production and methanogenic populations in an acidic West-Siberian
780 peat bog. *Environmental Microbiology*, **6**, 1159-1173.

781 Lähteenoja, O. and Page, S. (2011) High diversity of tropical peatland ecosystem
782 types in the Pastaza-Marañón basin, Peruvian Amazonia. *Journal of*
783 *Geophysical Research*, **116**, G02025

784 Lähteenoja, O., Ruokolainen, K., Schulman, L. and Oinonen, M. (2009) Amazonian
785 peatlands: an ignored C sink and potential source. *Global Change Biology*. **15**,
786 2311-2320.
787 Liebner, S., Zeyer, J., Wagner, D., Schubert, C., Pfeiffer, E.M. and Knoblauch, C.
788 (2011) Methane oxidation associated with submerged brown mosses reduces
789 methane emissions from Siberian polygonal tundra. *Journal of Ecology*. **99**, 914-
790 922.
791 Lofton, D.D., Whalen, S.C. and Hershey, A.E. (2014) Effect of temperature on
792 methane dynamics and evaluation of methane oxidation kinetics in shallow Arctic
793 Alaskan lakes. *Hydrobiologia.* **721**, 209-222.
794 Mauquoy, D., Blaauw, M., van Geel, B., Borromei, A., Quattrocchio, M., Chambers,
795 F.M. and Possnert, G. (2004) Late Holocene climatic changes in Tierra del Fuego
796 based on multiproxy analyses of peat deposits. *Quaternary Research.* **61**, 148-
797 158.
798 Mead, R., Xu, Y., Chong, J. and Jaffé, R. (2005) Sediment and soil organic matter
799 source assessment as revealed by the molecular distribution and carbon isotopic
800 composition of n-alkanes. *Organic Geochemistry* **36**, 363-370.
801 Megonigal, J.P. and Schlesinger, W. (2002) Methane-limited methanotrophy in tidal
802 freshwater swamps. *Global Biogeochemical Cycles*. **16**. 35-1
803 Mitsch, W.J., Nahlik, A., Wolski, P., Bernal, B., Zhang, L., Ramberg, L. (2010) Tropical
804 wetlands: seasonal hydrologic pulsing, carbon sequestration, and methane
805 emissions. *Wetlands ecology and management*. **18**, 573-586.
806 Moore, T. and Knowles, R. (1990) Methane emissions from fen, bog and swamp
807 peatlands in Quebec. *Biogeochemistry* **11**, 45-61.

Naafs, B.D.A., Inglis, G.N., Zheng, Y., Amesbury, M.J., Biester, H., Bindler, R., Blewett, J., Burrows, M.A., del Castillo Torres, D., Chambers, F.M., Cohen, A.D., Evershed, R.P., Feakins, S.J., Gałka, M., Gallego-Sala, A., Gandois, L., Gray, D.M., Hatcher, P.G., Honorio Coronado, E.N., Hughes, P.D.M., Huguet, A., Könönen, M., Laggoun-Défarge, F., Lähteenoja, O., Lamentowicz, M., Marchant, R., McClymont, E., Pontevedra-Pombal, X., Ponton, C., Pourmand, A., Rizzuti, A.M., Rochefort, L., Schellekens, J., De Vleeschouwer, F. and Pancost, R.D. (2017) Introducing global peat-specific temperature and pH calibrations based on brGDGT bacterial lipids. *Geochimica et Cosmochimica Acta* **208**, 285-301.

Naeher, S., Niemann, H., Peterse, F., Smittenberg, R.H., Zigah, P.K. and Schubert, C.J. (2014) Tracing the methane cycle with lipid biomarkers in Lake Rotsee (Switzerland). *Organic Geochemistry.* **66**, 174-181.

Nisbet, E., Dlugokencky, E., Manning, M., Lowry, D., Fisher, R., France, J., Michel, S., Miller, J., White, J. and Vaughn, B., Bousquet, P., Pyle, J.E., Warwick, N.J., Cain, M., Brownlow, R., Zazzeri, G., Lanoiselle, M., Manning, A.C., Gloor, E., Worthy, D.E.J., Brunke, E-J., Labuschagne, C., Wolff, E and Ganesan, A.L (2016) Rising atmospheric methane: 2007–2014 growth and isotopic shift. *Global Biogeochemical Cycles*. **30**, 1356-1370.

Page, S.E., Wűst, R., Weiss, D., Rieley, J.O., Shotyk, W. and Limin, S.H. (2004) A record of Late Pleistocene and Holocene carbon accumulation and climate change from an equatorial peat bog (Kalimantan, Indonesia): implications for past, present and future carbon dynamics. *Journal of Quaternary Sciences.* **19**, 625-635.

831 Pancost, R.D., Baas, M., van Geel, B. and Sinninghe Damsté, J.S. (2003) Response
832 of an ombrotrophic bog to a regional climate event revealed by macrofossil,
833 molecular and carbon isotopic data. *The Holocene* **13**, 921-932.
834 Pancost, R.D., Coleman, J.M., Love, G.D., Chatzi, A., Bouloubassi, I. and Snape, C.E.
835 (2008) Kerogen-bound glycerol dialkyl tetraether lipids released by
836 hydropyrolysis of marine sediments: A bias against incorporation of sedimentary
837 organisms? *Organic Geochemistry* **39**, 1359-1371.
838 Pancost, R.D., McClymont, E.L., Bingham, E.M., Roberts, Z., Charman, D.J.,
839 Hornibrook, E.R.C., Blundell, A., Chambers, F.M., Lim, K.L.H. and Evershed,
840 R.P. (2011) Archaeol as a methanogen biomarker in ombrotrophic bogs. *Organic*
841 *Geochemistry* **42**, 1279-1287.
842 Pancost, R.D. and Sinninghe Damsté, J.S. (2003) Carbon isotopic compositions of
843 prokaryotic lipids as tracers of carbon cycling in diverse settings. *Chemical*
844 *Geology* **195**, 29-58.
845 Pancost, R.D., Steart, D.S., Handley, L., Collinson, M.E., Hooker, J.J., Scott, A.C.,
846 Grassineau, N.V. and Glasspool, I.J. (2007) Increased terrestrial methane
847 cycling at the Palaeocene–Eocene thermal maximum. *Nature* **449**, 332-335.
848 Pancost, R.D., van Geel, B., Baas, M. and Damsté, J.S.S. (2000) $\delta^{13}C$ values and
849 radiocarbon dates of microbial biomarkers as tracers for carbon recycling in peat
850 deposits. *Geology* **28**, 663-666.
851 Quirk, M., Wardroper, A., Wheatley, R. and Maxwell, J. (1984) Extended hopanoids in
852 peat environments. *Chemical Geology* **42**, 25-43.
853 Raghoebarsing, A.A., Smolders, A.J.P., Schmid, M.C., Rijpstra, W.I.C., Wolters-Arts,
854 M., Derksen, J., Jetten, M.S.M., Schouten, S., Sinninghe Damste, J.S., Lamers,
855 L.P.M., Roelofs, J.G.M., Op den Camp, H.J.M. and Strous, M. (2005)

856 Methanotrophic symbionts provide carbon for photosynthesis in peat bogs.
857 *Nature* **436**, 1153-1156.
858 Rohmer, M., Bouvier-Nave, P. and Ourisson, G. (1984) Distribution of hopanoid
859 triterpenes in prokaryotes. *Microbiology* **130**, 1137-1150.
860 Rydberg, J., Klaminder, J., Rosén, P. and Bindler, R. (2010) Climate driven release of
861 carbon and mercury from permafrost mires increases mercury loading to sub-
862 arctic lakes. *Science of the Total Environment.* **408**, 4778-4783.
863 Sachse, D., Billault, I., Bowen, G.J., Chikaraishi, Y., Dawson, T.E., Feakins, S.J.,
864 Freeman, K.H., Magill, C.R., McInerney, F.A., Van der Meer, M.T., Polissar, P.,
865 Robins, R.J., Sachs, J.P., Schmidt, H-L., Sessions, A.L., White, J.W.C., West,
866 J.B and Kahmen, A. (2012) Molecular paleohydrology: interpreting the hydrogen-
867 isotopic composition of lipid biomarkers from photosynthesizing organisms.
868 *Annual Review of Earth and Planetary Sciences*. **40**. 221-249
869 Schuldt, R., Brovkin, V., Kleinen, T. and Winderlich, J. (2013) Modelling holocene
870 carbon accumulation and methane emissions of boreal wetlands: an earth
871 system model approach. *Biogeosciences* **10**, 1659-1674.
872 Segers, R. (1998) Methane production and methane consumption: a review of
873 processes underlying wetland methane fluxes. *Biogeochemistry* **41**, 23-51.
874 Sorensen, K.W. (1993) Indonesian peat swamp forests and their role as a carbon sink.
875 *Chemosphere.* **27**, 1065-1082.
876 Souto, M., Castro, D., Pontevedra-Pombal, X., Garcia-Rodeja, E. and Fraga, M.
877 (2016) Characterisation of Holocene plant macrofossils from North Spanish
878 ombrotrophic mires: vascular plants. *Mires and Peat*. **18**. 1-21

879 Souto, M., Castro, D., Pontevedra-Pombal, X., Garcia-Rodeja, E., Fraga, M.J. (2017)
880 Characterisation of Holocene plant macrofossils from North Spanish
881 ombrotrophic mires: bryophytes. *Mires and Peat*. **19**. 1-12
882 Summons, R.E., Jahnke, L.L. and Roksandic, Z. (1994) Carbon isotopic fractionation
883 in lipids from methanotrophic bacteria: relevance for interpretation of the
884 geochemical record of biomarkers. *Geochimica et Cosmochimica Acta* **58**, 2853-
885 2863.
886 Talbot, H.M., Bischoff, J., Inglis, G.N., Collinson, M.E. and Pancost, R.D. (2016a)
887 Polyfunctionalised bio- and geohopanoids in the Eocene Cobham Lignite.
888 *Organic Geochemistry* **96**, 77-92.
889 Talbot, H.M. and Farrimond, P. (2007) Bacterial populations recorded in diverse
890 sedimentary biohopanoid distributions. *Organic Geochemistry* **38**, 1212-1225.
891 Talbot, H.M., Handley, L., Spencer-Jones, C.L., Dinga, B.J., Schefuß, E., Mann, P.J.,
892 Poulsen, J.R., Spencer, R.G., Wabakanghanzi, J.N. and Wagner, T. (2014)
893 Variability in aerobic methane oxidation over the past 1.2 Myrs recorded in
894 microbial biomarker signatures from Congo fan sediments. *Geochimica et*
895 *Cosmochimica Acta* **133**, 387-401.
896 Talbot, H.M., McClymont, E.L., Inglis, G.N., Evershed, R.P. and Pancost, R.D. (2016b)
897 Origin and preservation of bacteriohopanepolyol signatures in Sphagnum peat
898 from Bissendorfer Moor (Germany). *Organic Geochemistry* **97**, 95-110.
899 Turetsky, M.R., Kotowska, A., Bubier, J., Dise, N.B., Crill, P., Hornibrook, E.R.,
900 Minkkinen, K., Moore, T.R., Myers-Smith, I.H. and Nykänen, H, Olefeldt, D.,
901 Rinne, J., Saarnio, S., Shurpali, N., Tuittila, E-S., Waddington, J.M., White, J.R.,
902 Wickland, K.P. and Wilmking, M (2014) A synthesis of methane emissions from

903 71 northern, temperate, and subtropical wetlands. *Global Change Biology* **20**,
904 2183-2197.
905 Väliranta, M., Korhola, A., Seppä, H., Tuittila, E.-S., Sarmaja-Korjonen, K., Laine, J.
906 and Alm, J. (2007) High-resolution reconstruction of wetness dynamics in a
907 southern boreal raised bog, Finland, during the late Holocene: a quantitative
908 approach. *The Holocene.* **17**, 1093-1107.
909 van Winden, J.F., Kip, N., Reichart, G.-J., Jetten, M.S.M., Op den Camp, H.J.M. and
910 Sinninghe Damsté, J.S. (2010) Lipids of symbiotic methane-oxidizing bacteria in
911 peat moss studied using stable carbon isotopic labelling. *Organic Geochemistry*
912 **41**, 1040-1044.
913 van Winden, J.F., Reichart, G.-J., McNamara, N.P., Benthien, A. and Sinninghe
914 Damsté, J.S. (2012a) Temperature-Induced Increase in Methane Release from
915 Peat Bogs: A Mesocosm Experiment. *PLoS ONE* **7**, e39614.
916 van Winden, J.F., Talbot, H.M., De Vleeschouwer, F., Reichart, G.-J. and Sinninghe
917 Damsté, J.S. (2012b) Variation in methanotroph-related proxies in peat deposits
918 from Misten Bog, Hautes-Fagnes, Belgium. *Organic Geochemistry* **53**, 73-79.
919 Volkman, J.K., Zhang, Z., Xie, X., Qin, J. and Borjigin, T. (2015) Biomarker evidence
920 for Botryococcus and a methane cycle in the Eocene Huadian oil shale, NE
921 China. *Organic Geochemistry* **78**, 121-134.
922 Wu, M.S., Feakins, S.J., Martin, R.E., Shenkin, A., Bentley, L.P., Blonder, B., Salinas,
923 N., Asner, G.P. and Malhi, Y. (2017) Altitude effect on leaf wax carbon isotopic
924 composition in humid tropical forests. *Geochimica et Cosmochimica Acta* **206**, 1-
925 17.

926 Xie, S., Nott, C.J., Avsejs, L.A., Maddy, D., Chambers, F.M. and Evershed, R.P. (2004)
927 Molecular and isotopic stratigraphy in an ombrotrophic mire for paleoclimate
928 reconstruction. *Geochimica et Cosmochimica Acta.* **68**, 2849-2862.
929 Yamamoto, S., Kawamura, K., Seki, O., Meyers, P.A., Zheng, Y. and Zhou, W. (2010)
930 Environmental influences over the last 16 ka on compound-specific $\delta^{13}C$
931 variations of leaf wax n-alkanes in the Hani peat deposit from northeast China.
932 *Chemical Geology* **277**, 261-268.
933 Yu, Z. (2012) Northern peatland carbon stocks and dynamics: a review.
934 *Biogeosciences* **9**, 4071-4085.
935 Yu, Z., Loisel, J., Brosseau, D.P., Beilman, D.W. and Hunt, S.J. (2010) Global peatland
936 dynamics since the Last Glacial Maximum. *Geophysical Research Letters* **37**.
937 Yvon-Durocher, G., Allen, A.P., Bastviken, D., Conrad, R., Gudasz, C., St-Pierre, A.,
938 Thanh-Duc, N. and del Giorgio, P.A. (2014) Methane fluxes show consistent
939 temperature dependence across microbial to ecosystem scales. *Nature* **507**,
940 488.
941 Zhao, Y., Yu, Z., Chen, F., Ito, E., Zhao, C. (2007) Holocene vegetation and climate
942 history at Hurleg Lake in the Qaidam Basin, northwest China. *Review of*
943 *Palaeobotany and Palynology.* **145**, 275-288.
944 Zheng, Y., Singarayer, J.S., Cheng, P., Yu, X., Liu, Z., Valdes, P.J. and Pancost, R.D.
945 (2014) Holocene variations in peatland methane cycling associated with the
946 Asian summer monsoon system. *Nature Commun*ications. **5**. 4631

947

948

949